TOPOLOGY ESTIMATION IN LOW VOLTAGE GRIDS USING WALLBOX CHARGING DATA RECORDINGS

Christian HOTZ
TH Köln – Germany
christian.hotz@th-koeln.de

Sergej BAUM
TH Köln – Germany
sergej.baum@th-koeln.de

Eberhard WAFFENSCHMIDT
TH Köln – Germany
eberhard.waffenschmidt@th-koeln.de

Ingo STADLER
TH Köln – Germany
ingo.stadler@th-koeln.de

Abstract

This paper presents an algorithmic approach to reconstructing topologies of low voltage grids based on e-vehicle charging station measurement data. Prerequisite is a sufficient penetration of the grid with smart meter equipped charging stations providing voltage and current measurements as well as communication infrastructure to exchange such data. The topology information thus obtained can facilitate a wide range of smart grid applications.

Introduction

Smart loads are a key component to solving the problem of an efficient power grid usage with a growing numbers and new types of electric loads. A decentralized control approach with communication among smart loads may avoid investments in a centralized control system. To allow plug-and-play capability of smart loads, it would be advantageous if they were able to detect the topology of the grid they are connected. Therefore, in this publication an algorithm to estimate the grid topology from coordinated voltage measurements of the smart devices is presented. It will be demonstrated with charging boxes for electric vehicles as typical exemplary controllable loads.

Papers with various approaches to solving this problem have been published in the past, they can be filed into three categories: Firstly, algorithms described in papers such as [1], [2] and [3] take advantage of different types of statistical analysis such as correlation coefficient matrices to determine electrical proximity between buses which is later processed into a qualitative grid topology, i.e. an adjacency matrix. This can be done using voltage measurements only but it is not possible to determine line impedances using this methodology. Other research [4], evaluates Power Line Communication data. Based on reflection and amplification properties of standing waves, physical lengths of lines are determined. A complete topology reconstruction including impedances using this technique is only possible for very simple grid layouts. The last and most common technology is matrix approximation including sparse recovery [5], [6]. For a series of voltage and current measurements, the node admittance matrix $\underline{\underline{Y}}$ is determined such that the RMS error of equation (1) is minimized over all measurement data:

$$\underline{I} = \underline{\underline{Y}} \cdot \underline{U} \qquad (1)$$

Admittance values below a threshold are then set to zero to obtain a sparse admittance matrix. This process reconstructs a grid including line admittances. It cannot reconstruct buses on which there are no measurements. In particular, it cannot reconstruct household connection lines which connect a building to the main grid line in its street.

The household connection line problem is addressed by the algorithm presented in this paper: it reconstructs a radial network, more specifically a binary tree. That includes inserting buses on which there are no measurements by approximating their location in the grid.

Simulation Environment: E-mobility management and optimisation - EMO

All research presented in this paper is based on a simulation environment specifically developed for low voltage smart grid application and e-vehicle charging algorithm research at TH Köln. Based on the Newton-Raphson power flow calculation tool PandaPower [7], the E-Mobility Management and Optimisation (EMO) simulation environment is implemented in Python. It includes fluctuating household loads and e-vehicle charging cycles from recorded timelines and/or load timeline generators [8], [9]. It also provides programming interfaces to implement smart charging algorithms including grid control and load management regimes such as P(U)-controls, P(I)-controls and predictive rolling horizon optimisation based on linear programming.

Identification of switch events and resulting Requirements to recorded Data

In a first step, we outline the required structure of the recorded measurements in the e-vehicle charging stations.

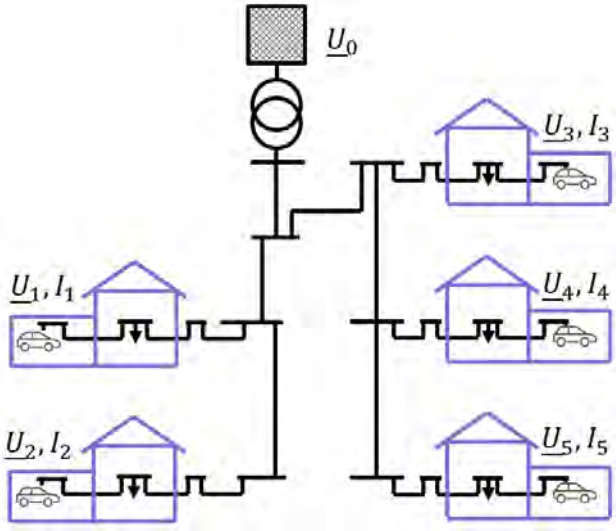

Figure 1: example grid used in the first part of the paper

For this paper, we assume symmetric three-phase charging as this is the most sensible technology for fast charging and thus deemed to prevail over currently common single-phase-charging technology in the long run. This makes it possible to use single-phase-equivalent-circuits. The results can, however, be transferred to single-phase systems. A power factor of $\varphi = 1$ is assumed for the charging process.

To describe the algorithm, we assume a simple topology with five households and five electric vehicles as depicted in figure 1. The algorithm was successfully tested on more complex grid topologies.

The topology estimation is based on a matrix of voltage drops $\Delta\underline{U}_i$ on buses resulting from load steps on buses ΔI_k: for each start and end of a charging cycle on a bus, in the further discussion referred to as Switch Events, the voltage drop on all Measurement Buses is determined (equation 2):

$$\Delta\underline{U}_i(\Delta I_k) = \underline{U}_i(t_0) - \underline{U}_i(t_1) \qquad (2)$$

Here, $\underline{U}_i$ is the complex voltage on a Measurement Bus i. The frames t_0 and t_1 are points in time before and after the Switch Event causing a current step ΔI_k on a charging bus k. An excerpt of an exemplary dataset is listed in table 1.

Time	Switch Event on Bus	$\frac{\Delta I}{A}$	$\frac{\Delta \underline{U}_1}{V}$	$\frac{\Delta \underline{U}_2}{V}$	…	$\frac{\Delta \underline{U}_n}{V}$
1:31 am	4	12,3	$1{,}1 \cdot e^{j44°}$	$1{,}2 \cdot e^{j41°}$	…	$0{,}3 \cdot e^{j44°}$
2:12 am	4	-9,3	$0{,}86 \cdot e^{j134°}$	$0{,}96 \cdot e^{j141°}$	…	$0{,}22 \cdot e^{j131°}$
2:44 pm	1	22,1	$0{,}4 \cdot e^{j29°}$	$0{,}4 \cdot e^{j34°}$	…	$1{,}4 \cdot e^{j43°}$
5:57 pm	2	18,2	$0{,}38 \cdot e^{j22°}$	$0{,}48 \cdot e^{j36°}$	…	$0{,}99 \cdot e^{j33°}$
…	…	…	…	…	…	…

Table 1: excerpt of a summary of Switch Events in a low voltage grid with electric vehicle charging stations

Interpretation of switch events: common lines

Dividing the voltage drop by the load step current yields an impedance value for every combination of two buses with measurement facilities (equation 3):

$$\underline{Z}_{CL,i,k} = \frac{\Delta \underline{U}_i(\Delta I_k)}{\Delta I_k};\ i,k \in [1 \dots 5] \qquad (3)$$

These impedances correspond to the impedance between the infinite grid which is approximated to be the connecting transformer to a higher voltage level (e.g. 10 kV/20 kV) and the common junction between said two buses furthest from this connecting transformer. These are henceforth referred to as Common Lines. Figure 2 illustrates their significance on the example grid from figure 1 for buses 3 and 4.

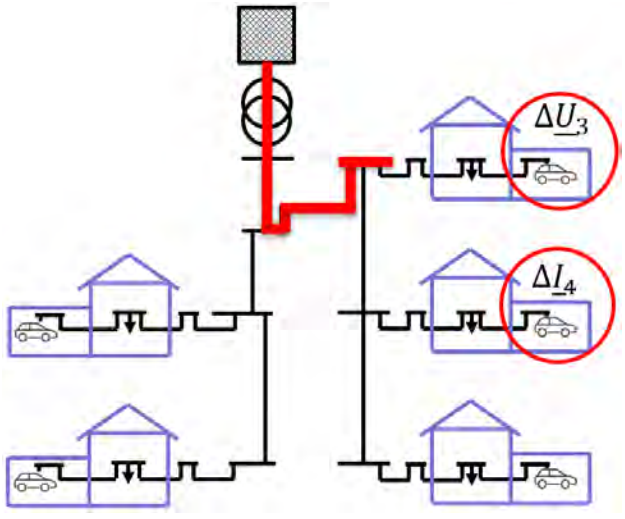

Figure 2: illustration of the concept of Common Lines

The red circles mark the bus on which the load step occurs and the bus on which the voltage measurements are recorded respectively. The section of the grid marked red constitutes the Common Line between those buses.

Determining this value for every combination of two buses yields a Common Line Matrix which is represented as a heatmap in figure 3 for reference (magnitudes only). Values on the main diagonal represent the entire distance between a bus and the connecting transformer and will later on be referred to as Self Impedances (equation 4).

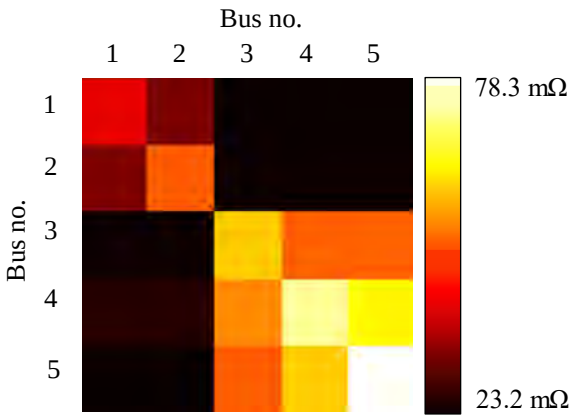

Figure 3: Common Lines Matrix (magnitudes) corresponding to the radial grid in figure 1; each element is calculated according to equation 3

$$\underline{Z}_{CL,self,i} = \frac{\Delta \underline{U}_i(\Delta I_i)}{\Delta I_i};\ i \in [1 \dots 5] \tag{4}$$

Reconstruction of the radial grid from common lines information

The information thus gained about Common Lines shared by any combination of two buses can now be processed to reconstruct the grid topology as a binary tree structure. To visualize the problem and its solution, figure 4 depicts a simplified and itemised block diagram corresponding to the grid shown in figure 1.

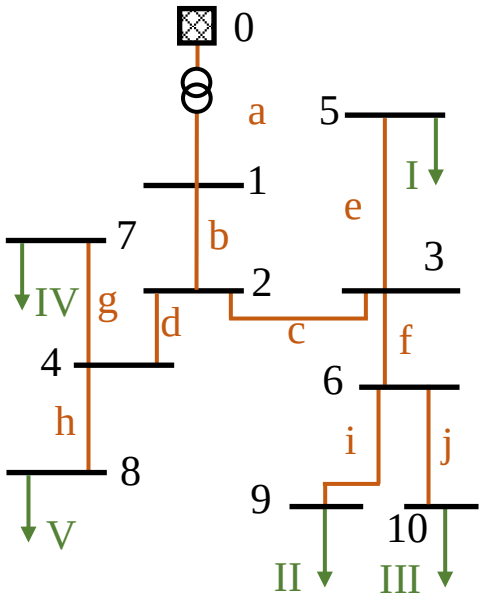

Figure 4: simplified and itemised block diagram corresponding to the grid shown in figure 1

Buses are depicted in black with Arabic numerals, line elements are drawn in purple and labelled with letters, the loads (and thus the Measurement Buses) are orange and labelled using Roman numerals.

As a first step to constructing the Estimated Admittance Matrix, a list of "Active Buses" is created. At the beginning of the algorithm, the list contains all Measurement Buses: I, II, III, IV, V. A list of the Common Line lengths for all combinations of two Active Buses is then made to find the "longest" element, i.e. the impedance item with the biggest real part, signifying the largest distance of the common junction to the connecting transformer. The values for the example are listed in table 2 (the values correspond to the data of the common line matrix in figure 3):

Combination of Measurement Buses	Real part of Common Line impedance
Buses I and II	14.48 mΩ
Buses I and III	14.48 mΩ
Buses I and IV	26.86 mΩ
Buses I and V	26.86 mΩ
Buses II and III	21.2 mΩ
Buses II and IV	14.46 mΩ
Buses II and V	14.46 mΩ
Buses III and IV	14.5 mΩ
Buses III and V	14.5 mΩ
Buses IV and V	36.01 mΩ

Table 2: Common Line elements for all combinations of active busses calculated using equation 3

The largest element, namely the Common Line impedance between Measurement Buses IV and V, is determined and five elements are added to the Estimated Topology:

- the Measurement Buses IV and V
- a Distribution Bus between Measurement Buses IV and V corresponding to Distribution Bus 4
- two reconstructed lines to connect Distribution Bus 4 to the two Measurement Buses IV and V corresponding to lines g and h

The impedance of the reconstructed lines g and h equals the self-impedance of the respective Measurement Bus it is connected to minus the Common Line impedance between the Distribution Buses. Example: The Self Impedance of Measurement Bus IV is the sum of the impedances of grid sections a, b, d, and g. The Common Lines impedance of Measurement Buses IV and V equals the sum of the impedances of sections a, b and d. The difference is the impedance of the household connection line IV (equations 5 for bus IV based on equations 3 and 4):

$$\underline{Z}_{CL,self,IV} = \underline{Z}_a + \underline{Z}_b + \underline{Z}_d + \underline{Z}_g \wedge$$
$$\underline{Z}_{CL,IV,V} = \underline{Z}_a + \underline{Z}_b + \underline{Z}_d \Leftrightarrow \qquad (5)$$
$$\underline{Z}_g = \underline{Z}_{CL,self,IV} - \underline{Z}_{CL,IV,V}$$

The Distribution Bus 4 is added to the list of Active Buses, the Measurement Buses IV and V are erased from the list. The remaining Active Buses are buses I, II, III and 4. A list of Common Line impedances between these elements is assembled. The Common Line impedance between the newly created Distribution Bus 4 and any other active element is the same as the Common Line impedance between

said element and either one of the Measurement Buses the Distribution Bus is connected to (equation 6):

$$\underline{Z}_{CL,x,4} = \underline{Z}_{CL,x,IV} = \underline{Z}_{CL,x,V}, x \in [I, II, III] \qquad (6)$$

The updated list is shown in table 3:

Combination of Measurement Buses	**Real part of Common Line impedance**
Buses I and II	14.48 mΩ
Buses I and III	14.48 mΩ
Buses I and 4	26.86 mΩ
Buses II and III	21.2 mΩ
Buses II and 4	14.46 mΩ
Buses III and 4	14.5 mΩ

Table 3: updated list of Common Line elements for all combinations of active buses

With the Common Line element between Measurement Bus I and Distribution Bus 4 constituting the largest resistance between any two Active Buses, these two Buses as well as a new Distribution Bus corresponding to bus 2 and its connection lines corresponding to lines c and d in figure 4 are added to the Estimated Topology.

The process is repeated until there is only one Active Bus left in the list. By connecting this last bus to the infinite grid via a line and a transformer, the Estimated Topology is completed. The results for the example configuration are plotted in figure 5.

The algorithm was able to successfully reconstruct the structure of the grid.

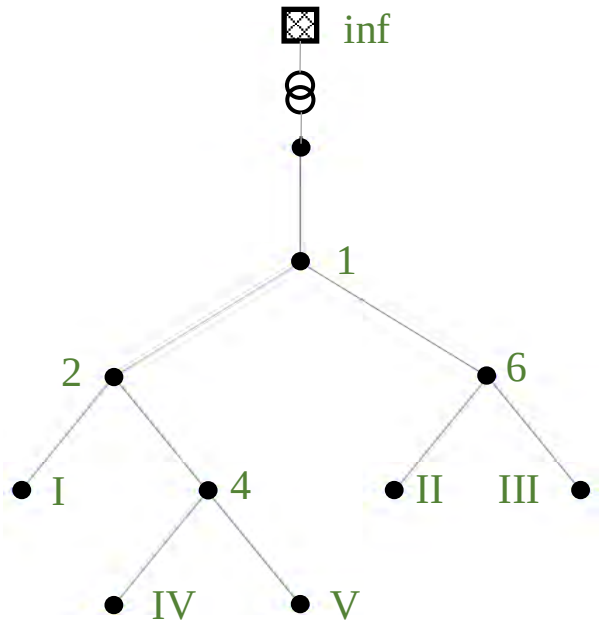

Figure 5: resulting Estimated Topology

Noise and Accuracy

Up to this point, the algorithm was tested on ideal simulation data. As a last step, we want to examine the accuracy of the algorithm under realistic circumstances. The main cause for deviation of the estimated impedances from the actual grid parameters in the Estimated Topology are any load fluctuations in the grid other than the examined load step of the Switch Event ΔI_k that affect the voltage drops $\Delta \underline{U}_j$ between the measurement frames t_0 and t_1. Such fluctuations are mainly caused by household loads and other electric vehicles. These influences are considered noise to the algorithm and are accounted for in the simulation environment by assigning load profiles to all household [8]. The shorter the

time between the Switch Event and the voltage measurement frames t_0 and t_1, the smaller the influence of the noise (cf.: equation 2). It is hence crucial to record voltage and current measurements frequently. A sampling rate of one measurement per minute was assumed for the following experiments.

To deal with these unpredictable fluctuations, Common Line impedance samples were derived from series of Switch Events. Two mechanisms of evening out noise were examined – median and average values of sets of $\underline{Z}_{CL}$-samples were compared regarding their accuracy.

Sets of 4, 10, 30, 60 and 120 Switch Events were produced, the respective method of noise cancelling applied, the topology estimated and the impedances of the Estimated Topology compared to the actual parameters of the grid.

Table 4 lists the RMS of the errors of the real and imaginary parts of all impedances for these cases. The study was conducted on a grid with 30 households equipped with 30 charging stations, 59 lines and 61 busses.

No. of Switch Events	**RMS error in impedance estimation over all impedances in grid**			
	Noise Cancelling using Median		Noise Cancelling using Average	
	Real	Imag.	Real	Imag.
4	68.3 %	333 %	75.9 %	506 %
10	19.9 %	43.4 %	133 %	483 %
30	5.5 %	10.0 %	94.1 %	302 %
60	4.5 %	9.4 %	54.2 %	144 %
120	4.5 %	7.9 %	30.3 %	90.5 %
240	4.2 %	7.7 %	21.7 %	67.3 %

Table 4: analysis of Topology Estimation accuracy under both noise cancelling regimes for various Switch Event dataset sizes

Quite obviously, the median is the superior noise cancelling method. Using the median, an RMS error of 10% or better can be achieved for both the real and the imaginary part of the impedance estimations with a Switch Event measurement sample set size of approximately 30 items. Figure 6 depicts common line matrices for a single Switch Event per Bus and a median over 120 Switch Events respectively to visualise the noise cancelling effect.

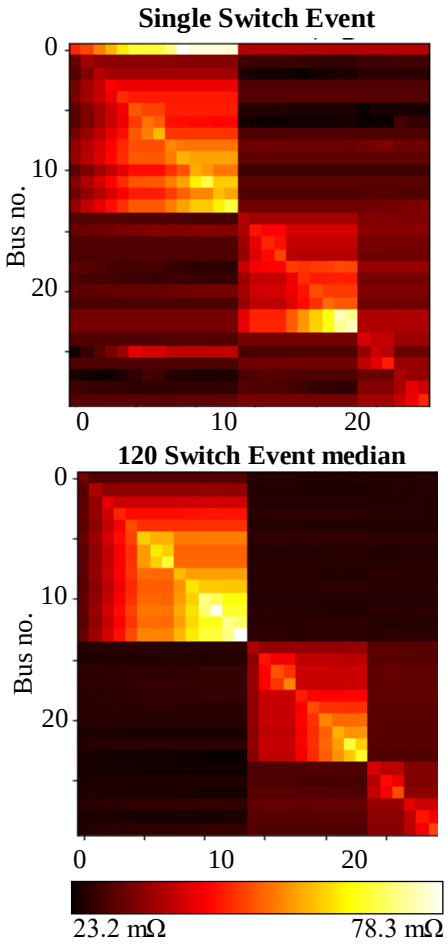

Conclusion

An algorithm to estimate the topology of a low voltage grid using measurement data recorded in e-vehicle charging stations was conceived, implemented and successfully tested on simulation data. In contrast to other algorithms presented in recent research, the algorithm is capable of determining Distribution Buses on which there are no measurements and include them into the reconstruction of the grid. The algorithm is susceptible to noise from fluctuating loads within the grid. Means of dealing with such noise were discussed. These means do, however, not apply to non-Gaussian disturbances, e.g. P(U)-controls which can be found in modern PV-VSIs and other inverter-coupled devices.

The algorithm reconstructs radial networks, which is a common topology for low voltage grids. If, however, the grid is meshed, the algorithm will yield incorrect results.

In conclusion, the presented algorithm yields the desired results with reasonable accuracy (an RMS error of less than 10% for 30 Switch Events in our example) and can, under consideration of undermining influences, be starting point for a variety of Smart Grid applications.

Acknowledgement

The Progressus project has received funding from the Electronic Components and Systems for European Leadership Joint Undertaking under grant agreement No 876868. This Joint Undertaking receives support from the European Union's Horizon 2020 research and innovation programme and Germany, Netherlands, Spain, Italy, Slovakia.

References

[1] Y. Weng, Y. Liao, and R. Rajagopal, "Distributed Energy Resources Topology Identification via Graphical Modeling," *IEEE Trans. Power Syst.*, vol. 32, no. 4, pp. 2682–2694, 2017, doi: 10.1109/TPWRS.2016.2628876.

[2] Y. Liao, Y. Weng, G. Liu, and R. Rajagopal, "Urban MV and LV Distribution Grid Topology Estimation via Group Lasso," *IEEE Trans. Power Syst.*, vol. 34, no. 1, pp. 12–27, 2019, doi: 10.1109/TPWRS.2018.2868877.

[3] J. Zhao, L. Li, Z. Xu, X. Wang, H. Wang, and X. Shao, "Full-Scale Distribution System Topology Identification Using Markov Random Field," *IEEE Trans. Smart Grid*, vol. 11, no. 6, pp. 4714–4726, 2020, doi: 10.1109/TSG.2020.2995164.

[4] I. Aouichak, K. Khalil, I. Elfeki, J.-C. Le Bunetel, and Y. Raingeaud, "Topology identification method for unknown indoor PLC home networks," in *2017 International Symposium on*

Electromagnetic Compatibility - EMC EUROPE: Angers, France, 4-7 September 2017, Angers, 2017, pp. 1–4.

[5] M. Babakmehr, M. G. Simoes, M. B. Wakin, A. A. Durra, and F. Harirchi, “Smart grid topology identification using sparse recovery,” in *2015 IEEE Industry Applications Society Annual Meeting*, Addison, TX, USA, 10/18/2015 - 10/22/2015, pp. 1–8.

[6] Z. Tian, W. Wu, and B. Zhang, “A Mixed Integer Quadratic Programming Model for Topology Identification in Distribution Network,” *IEEE Trans. Power Syst.*, vol. 31, no. 1, pp. 823–824, 2016, doi: 10.1109/TPWRS.2015.2394454.

[7] L. Thurner *et al.*, “Pandapower—An Open-Source Python Tool for Convenient Modeling, Analysis, and Optimization of Electric Power Systems,” *IEEE Trans. Power Syst.*, vol. 33, no. 6, pp. 6510–6521, 2018, doi: 10.1109/TPWRS.2018.2829021.

[8] N. Pflugradt and B. Platzer, “Behavior based load profile generator for domestic hot water and electricity use,” in *Innostock 12th International Conference, Lleida, Spain, 2012*.

[9] M. Sprünken, “Lastprofilgenerator für synthetische Ladeprofile für Elektromobilität,” Master Thesis, iet, TH Köln, Cologne, 2022.